

Analysis of intra-aortic balloon pump model with ovine myocardial infarction

Koyun miyokard enfarktüsünden intraaortik balon pompa modeli analizi

Mona Abdolrazaghi, Mahdi Navidbakhsh¹, Kamran Hassani², Shahram Rabban³, Hossein Ahmadi⁴

Department of Mechanical Engineering, Alberta University, Edmonton, Canada,

¹Department of Mechanical Engineering, Iran University of Science and Technology, Tehran,

²Department of Biomedical Engineering, Science and Research Branch, Islamic Azad University, Tehran

³Tehran Heart Research Center, Tehran

⁴Department of Cardiology, Tehran Medical University, Tehran, Iran

ABSTRACT

Objective: In this study, we have tried to model the effects of intra-aortic balloon pump (IABP) on myocardial infarction (MI) using the standardized data of MI in sheep which was obtained by ligation of the left anterior descending coronary artery.

Methods: Mathematical model of whole cardiovascular system was presented in accordance to the arterial tree. The lumped parameter model was primarily obtained for a rigid vessel regarding the vessel diameter. In this study, the proper lumped model of every vessel was obtained by incorporating the rigid vessel lumped model into the capacitance as a compliance of the vessel. Intra-aortic balloon pump was modeled with the hemodynamic parameters of the aorta. It was assumed that balloon pump inflates at the beginning of the diastole and deflates near the beginning of the next systole.

Results: During balloon pumping, the vessel diameter variation function counter pulsates sinusoidally with the same period of the cardiac cycle. End systolic pressure and end diastolic pressure decreases along with hemodynamic flow optimized through systemic arteries due to balloon pumping in diastole. It has been shown that the blood flow in subclavian artery increases as well. Moreover, the cardiac work keeps low, which prone to lower oxygen consumption. The results of modeling are in good agreement with IABP documentation.

Conclusions: The presented model is a useful tool for studying of the cardiovascular system pathology and the presented modeling data are in good agreement with the experimental ones. (*Anadolu Kardiyol Derg 2009; 9: 492-8*)

Key words: Mathematical modeling, myocardial infarction, cardiovascular system, intra-aortic balloon pump, animal, disease model

ÖZET

Amaç: Bu çalışmada, sol ön inen koroner arter bağlanması ile koyunlarda oluşturulan miyokard enfarktüsü (MI) standart verilerini kullanarak, MI'de intraaortik balon pompa (IABP) etkilerini model oluşturmak için çalışılmıştır.

Yöntemler: Tüm kardiyovasküler sistemin, matematiksel modeli arter ağacına göre sunuldu. Damar çapı dikkate alınarak rijidite için primer olarak lump parametre modeli elde edildi. Bu çalışmada, her damarın uygun lump modeli, rijid damar lump modeli sığasına eklenerek elde edildi. İntraaortik balon pompa aortanın hemodinamik parametreleri ile biçimleştirilmiştir. Balon pompası diyastol başında şişirildi ve sonraki sistolün başlangıcına yakın söndürüldü şeklinde tasarlandı.

Bulgular: Balonun pompalanması sırasında kalp siklusunun aynı periyodunda damar çapı değişim fonksiyonu sinuzoidal olarak tersine pulsasyon gösterdi. Diyastoldeki balon pompalanması dolayısı ile sistemik arterlerde hemodinamik akım optimizasyonu ile birlikte sistol sonu ve diyastol sonu basınç azalır. Subklavyen arterde de kan akımının arttığı gösterildi. Ayrıca, kalp işi, daha az oksijen tüketimine eğilim gösterecek şekilde düşüktür. Biçimlenmenin sonuçları IABP dokümantasyonla iyi uyumaktadır.

Sonuç: Sunulmuş olan model, kardiyovasküler sistem patolojisi çalışmaları için yararlı bir araçtır ve sunulan model verileri deneysel olanlarla iyi bir uyum göstermektedir. (*Anadolu Kardiyol Derg 2009; 9: 492-8*)

Anahtar kelimeler: Matematik biçimlendirme, miyokard enfarktüsü, kardiyovasküler sistem, intraaortik balon pompası, hayvan, hastalık modeli

Introduction

Ischemic heart disease now afflicts millions of people and is the significant cause of death in contemporary life. Ovine is mostly used in cardiovascular disease experiments particularly myocardial infarction (MI) due to the physiological and anatomical similarities with human being. In the recent paper, the standardization of MI in sheep has been shown by occluding coronary arteries (1). In this research, mathematical model of MI and intra-aortic balloon pump (IABP) were presented according to the ovine-MI data collected in the laboratory.

There are scientists who worked on mathematical modeling of cardiovascular system (2-6). The use of intra aortic balloon pumping (IABP) in acute myocardial infarction has provided a new dimension in the therapy of this pathology. Dunkman et al. (7) presented clinical and hemodynamic results of intra aortic balloon pumping and surgery for cardiogenic shock. In 2000 the intra aortic propeller pump, a new device designed to continuously reduce after load, was developed (8). Then, Dekker, et al. (9) compared the efficiency of a new propeller pump to provide hemodynamic support to the IABP in an acute mitral regurgitation animal model. Masi, et al. (10) presented the first case of a patient with sudden thrombosis of an abdominal aortic aneurysm after removal of an IABP. We have tried to take a slightly different approach to the mathematical modeling of cardiovascular system and exhibit the effects of IABP on MI using the experimental data which was obtained from sheep and present the results by different graphs extracted from the mathematical model. To realize this aim, this study includes the following components (11-24):

- 1- The experimental data, which were used for the model.
- 2-The mathematical method which was used to present the cardiovascular system operation (11, 12, 14-16, 21).
- 3-The mathematical modeling of IABP and inserting the effects into the model using the experimental data (13, 24).
- 4-The study of IABP on MI using the mathematical model of cardiovascular system.

The main purpose of our research was to present a model to be used by medical doctors to enable them to observe the effects of IABP on MI for each patient.

Methods

In this section, first the method of inducing MI in sheep is explained. Then, we have obtained the lumped parameter model for elastic vessel in accordance to the arteries' diameter. Then whole cardiovascular system regarding obtained model is developed. Next, sheep-MI data is applied for modeling the ischemia. Finally, the IABP is modeled for treating the disease and stabilizing the patient's conditions.

All experiments were performed with permission of ethical committee of Tehran Heart Research Center and received humane care in accordance with the 'Guide for the Care and

Use of Laboratory Animals' published by the US National Institute of Health (NIH publication no. 85-23, revised 1996).

Twelve Iranian ewes weighing 40 - 60 kg were used. MI was induced by ligation of the main diagonal branch of the left anterior descending (LAD) coronary artery (namely homonymous artery in sheep). The procedure of operation started after the chest opened by left lateral thoracotomy incision, the second diagonal branch of the LAD was ligated at a point approximately 40% distant from its base.

Cardiac function was evaluated preoperatively and on the 1st postoperative day using transthoracic echocardiography (Toshiba model SSA380A, Toshiba Corporation, Tochigi-ken, Japan). The following parameters were measured: left ventricular end-diastolic dimension (LVEDD), left ventricular end-systolic dimension (LVESD), fractional shortening (FS) and ejection fraction (EF). Fractional shortening was defined as $LVEDD - LVESD / LVEDD$ and EF was defined as $LVEDD - LVESD / LVEDD$ (13).

Electrocardiograms (ECG) were continuously displayed on a monitoring system (SPACELAB, Spacelabs Medical Inc., Redmond, WA, USA) and intermittently obtained on a paper chart record. By peripheral cannulation of an artery in the ear, systemic arterial pressure was continuously monitored. The left jugular vein was cannulated with a heparin-coated catheter (Arrow International, Reading, PA, USA) and the central venous pressure (CVP) was measured. Measurements were recorded preligation and 1 hour postinfarction. Successful ligation was confirmed by myocardial cyanosis and hypokinesia with bulging and ST-segment changes on the electrocardiogram.

Echocardiographic and electrocardiographic measurements were done before the surgery, also repeated 1 day and 2 months after the surgery. For modeling the pathology condition, we used two-month data of heart in infarction condition due to the stability and irreversibility of the results (1).

Statistical analysis

Data analysis was carried out by SPSS software version 12.0 (SPSS Inc, Chicago, IL, USA). Each variable was evaluated by Student's paired t-test. P values < 0.05 were considered statistically significant. All data are presented as mean \pm standard error of mean unless otherwise specified (1).

Mathematical model of cardiovascular system in normal and MI condition (21, 24)

Olufsen et al. (17) used the equations of fluid dynamics to derive a number of lumped models for blood flow and pressure in the systemic arteries. He started with the one-dimensional Navier-Stokes equations describing time-dependent flow and pressure in a rigid vessel and derived first- and second-order lumped models using Laplace transform. The resulting lumped models can be represented by electrical circuits. The most popular of the lumped models is the three-element Windkessel model with two resistors and a capacitor according to Figure 1 (a) and 1(b). An inducer is seen in the figure representing the inertia of blood. The differential equation can be represented for the circuit, which was shown in Figure 1, as:

$$L_1 \left(\frac{1}{R_1} + \frac{1}{R_2} \right) \frac{dq}{dt} + q = \frac{1}{R_2} \left(\frac{L_1}{R_2} \frac{dp}{dt} + p \right) \quad (1)$$

Where the values for the inductance (L1) and the resistances (R1), (R2) as functions of the artery and fluid properties:

$$L_1 = (\lambda_q - \lambda_p) \frac{8\rho L}{\pi R_2}; R_1 = \left(\frac{\lambda_q}{\lambda_p} - 1 \right) \frac{8\mu L}{\pi R_4}; R_2 = \frac{8\mu L}{\pi R_4} \quad (2)$$

Note that the pressure p(t) actually represents the pressure difference between the inlet and outlet of the artery and q(t) represents the blood flow. The values of time-scale λ_p and λ_q depend on the radius of the artery (R). It shall be noted if the radius of the artery is less than 0.2 cm, the circuit has only one

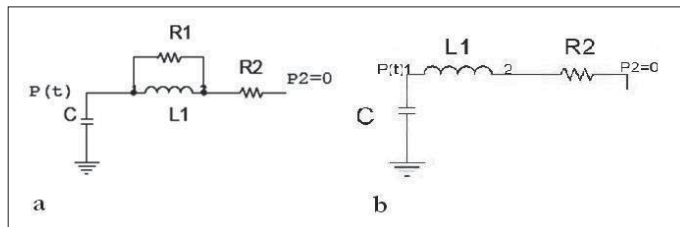


Figure 1. a: Equivalent lumped parameter model for elastic vessel with radius more than 0.2 cm and less than 1.5 cm. b: Equivalent lumped parameter model for elastic vessel with radius less than 0.2 cm and also for the rest of cardiovascular system including arterioles, capillaries, systemic veins, pulmonary arteries, and veins, left and right heart

resistor but there are two resistors in the circuit for the arteries with the radius of more than 0.2 cm. Furthermore, the value of time-scale is determined according to the following relations:

If radius of the artery is less than 0.2 cm then $\lambda_q = 0.1729$; $\lambda_p = 0.0075$

If radius of the artery is more than 0.2 cm then $\lambda_q = 0.2057$; $\lambda_p = 0.0392$

As we know, the arteries are compliant therefore, the value of (C) should be calculated. We used another mathematical method to calculate the compliance parameter mentioned in the circuit which is differ than the Olufsen method and it will be discussed in the next part. The electrical diagram of the cardiovascular system is illustrated in Figure 2. The diagram consists of 43 compartments representing whole cardiovascular system. We have detailed the arterial tree and included the main arteries in the diagram. Each compartment consists of three elements including a capacitor, an inducer and one or two resistors. The number of resistor in each compartment depends on the artery radius as discussed in Olufsen model. The values of (L₁), (R₁) and (R₂), for each artery, were calculated using the relation 2. In order to calculate the compliance of the arteries (C), the following equation was applied which (r) represents the artery radius, (h) is the thickness, (Δz) is the length of the artery and (E) refers to the Yung module of elasticity. The anatomical data of each artery were extracted from the physiological references (2).

$$C = \frac{3\pi \cdot r^3 \Delta z}{2 Eh} \quad (3)$$

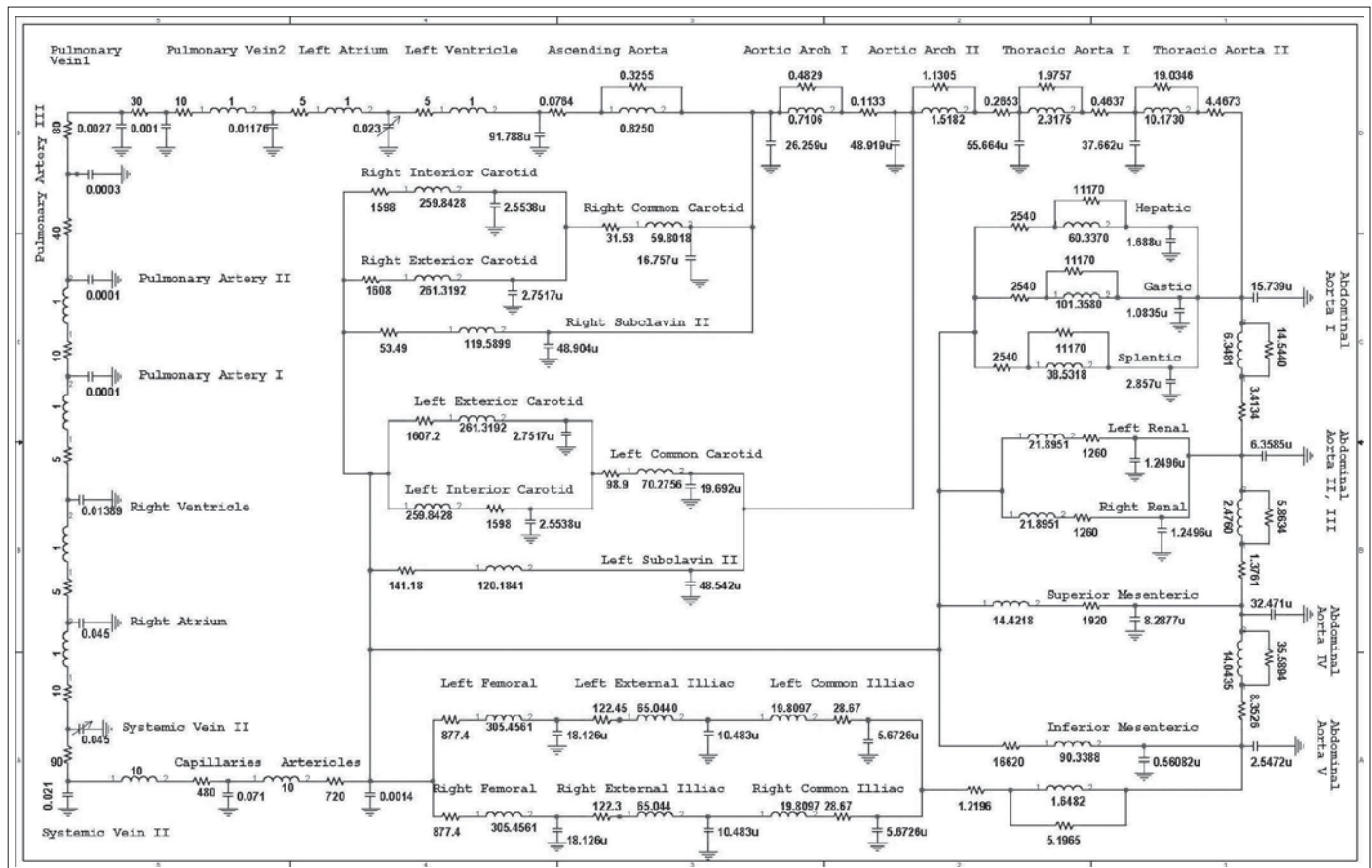


Figure 2. The equivalent analog electric model of whole cardiovascular system

The values of the hemodynamic parameters for ventricles, pulmonary artery, veins, arterioles, capillaries, and atriums were extracted from the literature (2, 20).

The heart rate was assumed 75 beats per minute and the cardiac cycle is 0.8 second. This model can be divided into two main parts: the heart, including atriums and ventricles, and the arterial system. To facilitate the understanding of the system, we have brought the anatomic structures into the circuit. The first part, which branches after the aortic arch I includes the main brain and hands arteries. The second part includes aorta, mesenteric, renal, gastric, hepatic and splenic arteries. The feet arteries including femoral and iliac are shown in the lower part of the circuit. The current, blood flow, passes through the arteries and all the branches reach at the point before the arterioles. The arterioles, capillaries, and systemic veins are presented by three compartments. The rest of the circuit includes left and right ventricles/atriums and pulmonary circulation. In order to present the operation of the heart in the model, we collected the data of 12 sheep before infarction and two months later. The data enabled us to model the operation of cardiovascular system both in normal and in MI condition, which is shown in Table 1 (1).

Central venous pressure shows right atrium pressure to equalize the right and left atrium pressure (2), therefore we have assumed that left atrium pressure and end diastolic pressure values are approximately the same as central venous pressure. Furthermore, end systolic pressure was assumed to have same value as systemic arterial pressure.

Firstly, we calculated the essential parameters for modeling of cardiovascular system in normal condition. Total heart period in normal condition is 0.76 sec (corresponding to 60/78.7) when the ejection- fraction (EF) of ventricle is 71.64%, and left ventricle volume (QLV) has the maximum volume of 46.48 ml. Then the stroke volume is $0.7164 \times 46.48 = 33.3$ (EF \times QLV_{max}) or $71.64 - 46.48 = 33.1$ (QLV_{max} - QLV_{min}).

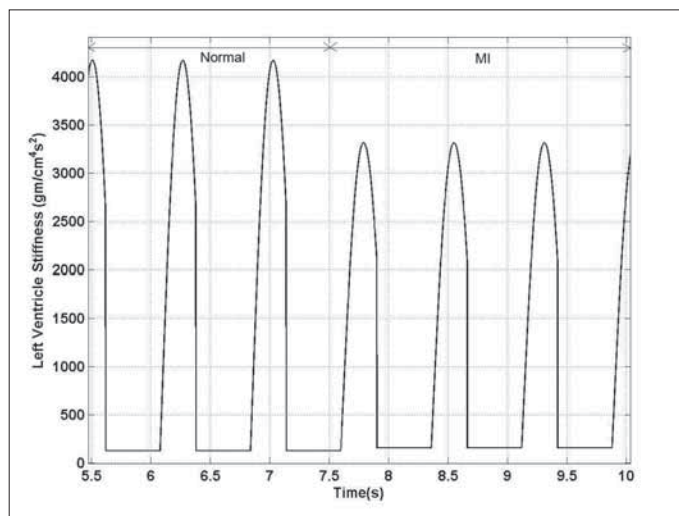


Figure 3. Model of left ventricle stiffness

Using this amount of stroke volume and assuming 0.76 sec for cardiac period, we calculated the average ventricular outflow (cardiac output) as $33/0.76 = 43.42$ ml/s. Considering (2) the atrium pressure (P_{AT}) equal to 4.5 mmHg, left ventricle pressure in systole (P_{ES}) to 90 mmHg, we calculated the systolic and diastolic left ventricle stiffness as follows:

$$S_{LD} = PAT \times 1332 / QLV_{max} = 123.23 \text{ gm} / \text{cm}^4\text{s}^2 \quad (1)$$

At the end of the systole, the systolic maximum stiffness is :

$$S_{LD} = PES \times 1332 / QLV_{min} = 4058 \text{ gm} / \text{cm}^4\text{s}^2 \quad (2)$$

the values for the ischemic condition were obtained by the same procedure. The heart period changes to 0.82 sec (60/72.8). The stroke volume was calculated 31.28 ml by considering EF equal to 58.57%, and maximum left ventricle volume equal to 53.25, ($0.5857 \times 53.25 = 31.28$). Also, stroke volume decreases to 31.67 ml (53.25 - 21.58). Systolic stiffness and diastolic stiffness were calculated 155.1 gm/cm⁴s² ($6.1 \times 1332 / 53.25$), and 3160.26 gm/cm⁴s² ($51.2 \times 1332 / 21.58$) respectively.

It is also assumed that the systolic time lasts for 0.3 seconds, and diastolic time lasts 0.5 seconds in both normal and ischemic condition.

The ventricles were modeled by a single varying compliance, the same as a muscle, which relaxes or expands during a heart cycle. It is also assumed that the systolic time lasts for 0.3 seconds, and diastolic time lasts 0.5 seconds. The ventricles' activation function is generated by a step-function, U(t), with pulse width of 39.5% corresponding to 0.3/0.76 (systolic time/total time), with unit amplitude. During systole, the sinusoid function, with amplitude equal to ventricle stiffness, is multiplied by the activation function make cardiac stiffness function noting that the frequency is 7.85 Hz ($2\pi/0.8$). Equations 3 and 4 show the proper stiffness relations for left and right ventricles respectively.

$$S_{LV} = 1/C_{LV} = (S_{LS} \sin(\frac{2\pi}{T}) + S_{LD}).U(t) \quad (3)$$

$$S_{RV} = 1/C_{RV} = (S_{RS} \sin(\frac{2\pi}{T}) + S_{RD}).U(t) \quad (4)$$

In MI condition, the proper values should be substituted in 8th second in the model. Figure 3 shows the stiffness variation versus time due to MI.

The intra-aortic balloon pump modeling (21)

Figures 4, 5 illustrate the equivalent lumped model of IABP. IABP was inserted in the model between descending aorta and thoracic aorta. The balloon operates one time in each heart cycle. In the diastole phase, the balloon expands and it contracts near the next systole phase. The function, R(x), describing the variation of the artery radius was formulated by a sinusoid function, which varies between 1 cm to 1.5 cm in diastole and it keeps constant at 1 cm in systole. The electrical model describing

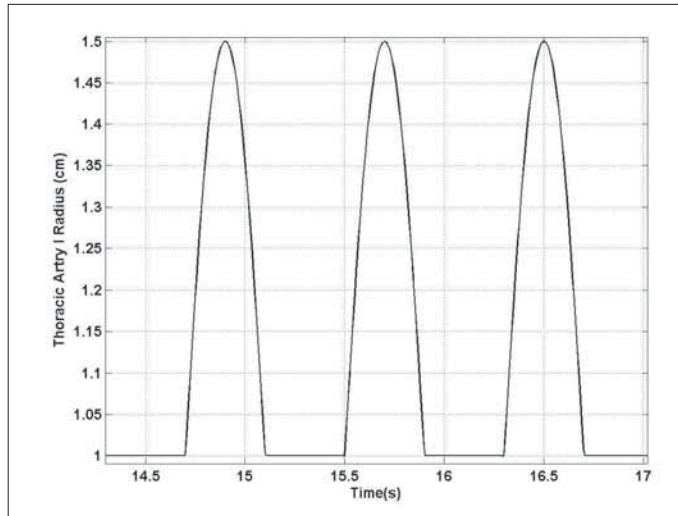


Figure 4. Thoracic artery radius changes due to applying IABP
IABP - intra-aortic balloon pump

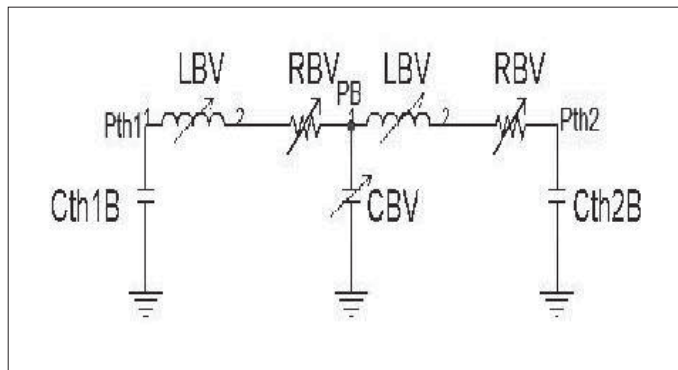


Figure 5. Equivalent intra-aortic balloon pump lumped model

IABP should be noted in Figure 5 once again where CBV refers to the varying compliance due to balloon pumping, RBV is varying resistance due to balloon pumping and LBV is varying inductance. We assumed the varying compliance of IABP is the average of the thoracic I compliance (Cth1) and the thoracic II (Cth2). Furthermore, the new values of thoracic I, II compliances during balloon pumping, Cth1B and Cth2B, were assumed half of the initial values. In the same method, the values of RBV and LBV were calculated in accordance with the following relations:

$$CB = \frac{Cth1 + Cth2}{2}; CBV = CB \cdot (Rx)^3 \quad (8)$$

$$Cth1B = (Cth1) / 2; Cth2B = (Cth2) / 2 \quad (9)$$

$$RB = Rth1/2; RBV = \frac{RB}{(Rx)^4} \quad (10)$$

$$LB = Lth1/2; LBV = \frac{LB}{(Rx)^2} \quad (11)$$

Note that (Rth1) is thoracic I resistance and (Lth1) is thoracic I inductance. R(x) is the varying artery's radius function.

Results

The hemodynamic values of the model are obtained for ischemic bluish discoloration and hypokinesia in the cardiac tissue in an area of 30x40mm.

In this section, we demonstrate the pressure-time and volume-time graphs of aorta and the effect of balloon pumping on the graphs in a defined ischemic area.

The detailed of mathematical modeling of cardiovascular system and intra-aortic balloon pump data in our previous studies which we have discussed both normal and MI conditions of cardiovascular system, and proved the result with the clinical data (21, 24).

Figure 6 demonstrates thoracic aorta I pressure versus time during normal, MI and balloon pumping conditions. The peak in systole is 65 mmHg but decreases to 60 mmHg due to MI. When IABP is applied, the systole pressure reaches to nearly 70

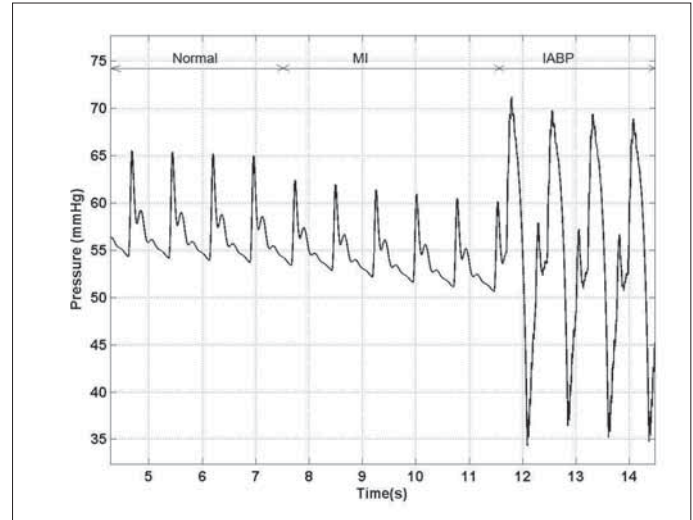


Figure 6. Model thoracic aorta pressure curve during normal, MI, and IABP conditions

IABP - intra-aortic balloon pump, MI - myocardial infarction

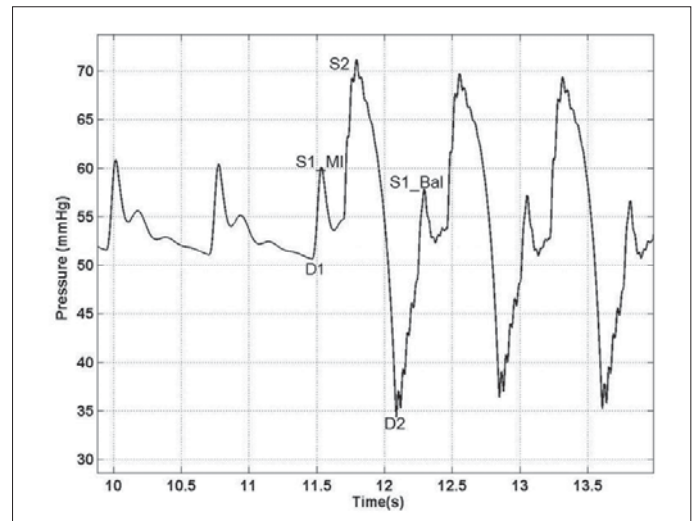


Figure 7. Model thoracic aorta pressure curve during MI, IABP conditions

IABP - intra-aortic balloon pump, MI - myocardial infarction

mmHg. The difference between systole and diastole pressures is 35 mmHg in IABP condition comparing to 10 mmHg in normal/MI condition. The effects of balloon pumping are presented in figure 7 more precisely. During balloon counter pulsation, a double-hump and dip pattern is notified. The first hump is end-systolic pressure (ESP). It is clearly observable that the ESP is decreased after balloon pumping. End-systolic pressure decreases to 60 mmHg when balloon is applied (point S1-Bal). The second hump happens in diastole is peak diastolic pressure (PDP) due to balloon inflation in point S2. It increases 10 mmHg more than ESP. End-diastolic pressure (EDP) is decreased lower than normal value, almost 20 mmHg. End-diastolic pressure is decreased from 50 mmHg (point D1), to 35 mmHg in point D2, when IABP is applied.

Figure 8 shows a real electrocardiogram and IABP waveforms, which were recorded from a 66 year-old patient (2). Second peak is produced by balloon inflation and ideally raises diastolic pressure higher than the systolic pressure. The first dip is due to the time when aortic valve is close. The second dip relates to balloon deflation just before next systole, which is like "V" in shape.

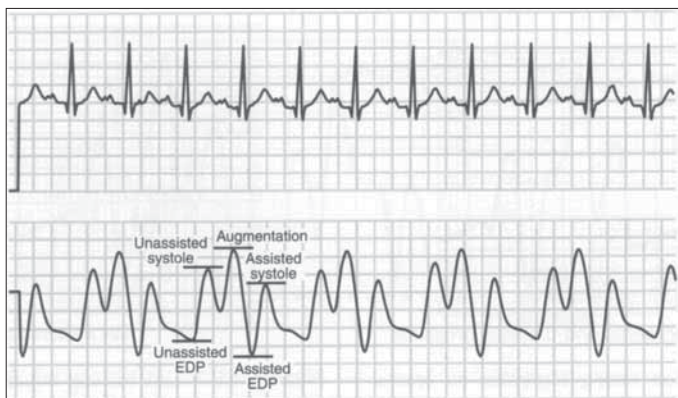


Figure 8. Electrocardiogram tracing and measured thoracic aorta pressure curve during MI, IABP (1:2) conditions for a sample documentation of IABP waveform of aortic pressure of the study

IABP - intra-aortic balloon pump, MI - myocardial infarction

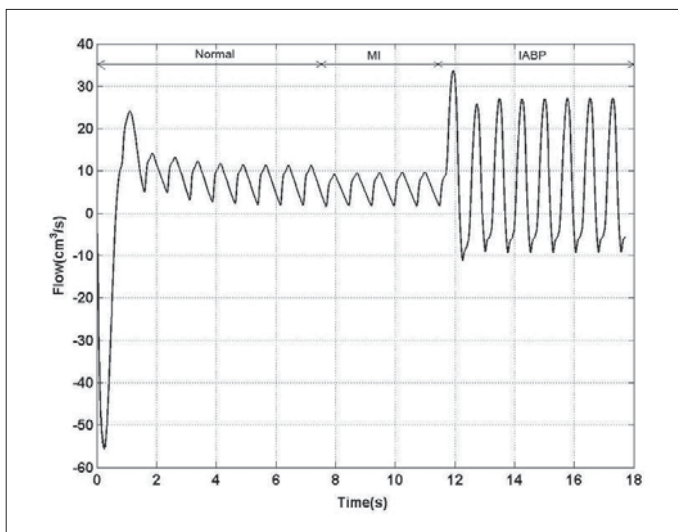


Figure 9. Model subclavian II flow during normal, MI and IABP conditions

IABP - intra-aortic balloon pump, MI - myocardial infarction

Deflation of the balloon reduces EDP by approximately 15 mmHg and lowers systolic pressure (assisted systolic pressure) by 5 to 10 mmHg the same as the points S2 and S1-Bal in Figure 7.

Left subclavian II flow is shown in figure 9 during normal, MI, and IABP conditions. The aorta flow decreases due to MI but the rate is very small. The flow increases approximately by 15cm³/s when IABP was applied.

Left ventricle work decreases dramatically due to MI in figure 10. Also, during balloon pumping, the cardiac work decreases and does not return to its normal value.

Discussion

Along with experimental animal model done for investigating the effect of several medicines, stem cells, there are also some possibilities to study the hemodynamic treatment of the disease without performing with experiments, through mathematical modeling. In our previous study, our standardization in MI has expressed the pathologic viewpoint of acute ischemia (1), and in this present study, the mathematical modeling of MI has been studied and its treatment through applying IABP.

The validation of the model has already been confirmed for both normal and MI condition (21, 24). All the pressure-time and volume-time graphs belonging to the different parts of the cardiovascular system can be obtained from the model and they are in complete agreement with the physiological data.

As we have shown in result section, when MI occurred the contractility of the left ventricle decreased which caused to decline in both left ventricle and systemic pressure. The reduction of left ventricle pressure is completely verified by the previous studies (2).

During applying, IABP circulatory benefits occur during both systole and diastole. Balloon inflation at the onset of diastole increases aortic diastolic pressure to a level close to systolic pressure and also displaces blood volume equal to its inflation volume. As in previous section, subclavian II aorta flow, a systemic aorta flow has shown that blood flow increases due to balloon inflation at diastole.

Deflation of the balloon occurs at the end of isovolumetric contraction (just before opening of the aortic valve) and is

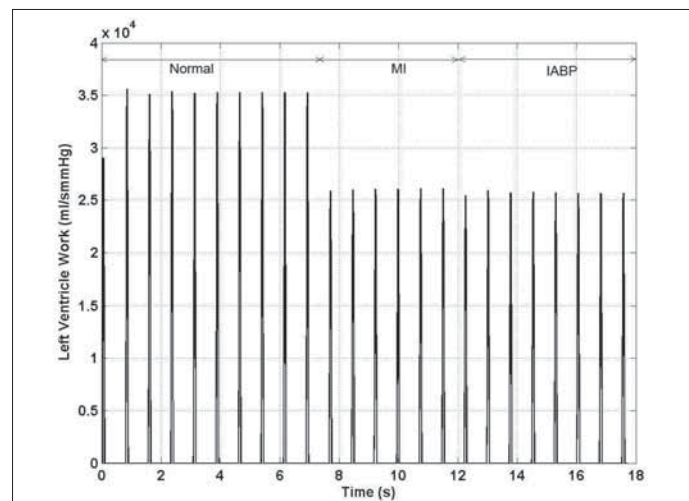


Figure 10. Model left ventricle work during normal, MI and IABP conditions

IABP - intra-aortic balloon pump, MI - myocardial infarction

maintained the onset of diastole. The studies show that the rapid diastolic inflation of the balloon and displacement of blood leaves a void (proportional to the size of the balloon) when the balloon deflates. Therefore, a potential intra-aortic vacuum is created that decreases aortic EDP below the patient's baseline value (2).

In previous section, we showed that EDP and ESP of aortic pressure are both decreased after applying IABP, which demonstrates the preload and afterload decreases relatively. According to the arterial systemic graph during balloon pumping, there are two pressure responses that are influenced by the deflation timing, first, the aortic end-diastolic pressure, following the balloon inflation/deflation cycle, should be lower than the preceding unassisted aortic end-diastolic pressure. This event should be V shaped, should also be the lowest point on the IABP-assisted and unassisted blood pressure curves. Second, the systolic peak that occurs after the balloon inflation/deflation cycle should be lower than the previous unassisted systolic peak. There are a couple of benefits, first, decreased resistance to opening the aortic valve and left ventricular ejection (decreased afterload) decreased myocardial work and Oxygen consumption (2). Not surprisingly, according to the obtained results cardiac work keeps low after balloon pumping. It should be noted that we wanted to compare all the parameters and values among normal, MI and IABP conditions therefore only mean values have been considered for modeling and the standard deviations values were not considered. This can be a study limitation for our work.

Conclusively, the model has been well proved in normal, MI, and IABP conditions with previous studies. By confirming our model with ovine model, we could calibrate and examine the model very well in cardiac part with living system. Therefore, the model could be applied very well for diagnosis, treatment of some cardiovascular diseases such as coronary by pass, aortic aneurysm, stenosis. Furthermore, the model could be completed with addition of control system, which could reflect neural reaction in cardiovascular system.

At last, as the results of modeling are based on the standardization done for ischemic bluish area, the model could be considered as a mathematical model for standardized MI.

Study limitations

The major limitation of the study is the low number of the ovine used for sampling. We are working with more numbers now to improve our results. The other limitation relates to the mathematical model because it does not operate completely the same as human cardiovascular system and it is a model, which mimics the general specifications of the cardiovascular system.

Conclusions

We tried to present a mathematical model, which exhibits the effects of IABP on MI using the hemodynamic data extracted from sheep. The results of modeling showed agreement with relevant clinical data and we think the model is a useful tool for studying the operation of cardiovascular system in normal condition and investigating the relevant pathologies.

References

1. Rabbani SH, Ahmadi H, Fayazzadeh E, Sahebjam M, Boroumand M, Sotudeh M, et al. Development of an ovine model of myocardial infarction. *J ANZ Surgery* 2008; 78: 78-81.
2. Rideout VC, Mathematical and computer modeling of physiological system. New Jersey: Printice-Hall Inc; 1991.
3. Beeler G.W, Reuter H. Reconstruction of the action potential of the ventricular myocardial fibers. *J Physiol* 1977; 268: 177-210.
4. Manoliu V. Consideration about the lumped parameter windkessel model applicativity in the cardiovascular system structure. Proceedings of the National Symposium of Theoretical Electrical Engineering, SNET'04. 22-23 October, 2004. Burcharest; UPB: p. 428-37.
5. Waite L. Biofluid mechanics in cardiovascular system. McGraw-Hill's Biomedical Engineering Series. New York: McGraw-Hill; 2006.
6. Hassani K, Navidbakhsh M, Rostami M, Simulation of the cardiovascular system using equivalent electronic system. *J Biomedical Paper* 2006; 150: 105-12.
7. Dunkman W, Leinbach R.C, Buckley MJ, Mundth ED, Kantrowitz AR, Austen WG, et al. Clinical and hemodynamic results of intra aortic balloon pumping and surgery for cardiogenic shock. *J Circ* 1972; 46: 465-77.
8. Reitan O, Sternby J, Ohlin H. Hemodynamic properties of a new percutaneous intra aortic axial flow pump. *ASAIO Journal* 2000; 46: 323-9.
9. Dekker A, Reesink K, van der Veen E, Van Ommen V, Geskes G, Soemers C, et al. Efficiency of a new intra aortic propeller pump vs the intraaortic balloon pump (an animal study). *Chest* 2003; 123: 2089-95.
10. Masi M, Mees U, Vandekerckhof J, Hendriks M. Acute thrombosis of an abdominal aortic aneurysm following intra-aortic balloon pumping. *J Interact Cardiovasc Thorac Surg* 2007; 658-60.
11. Rupnic M, Runvovc F, Sket D, Kordas M. Simulation of steady state and transient phenomena by using the equivalent electronic circuit. *Comput Methods Programs Biomed* 2002; 67: 1-12.
12. Liang F, Liu H. A closed-loop lumped parameter computational model for human cardiovascular system. *JSME International Journal Series C* 2005; 48: 484-93.
13. Takeuchi K, Nohtomi Y, Yoshitani H, Miyazaki C, Sakamoto K, Yoshikawa J. Enhanced coronary flow velocity during intra-aortic balloon pumping assessed by transthoracic Doppler echocardiography. *J Am Coll Cardiol* 2004; 43: 368-76.
14. Westerhof N, Bosman F, DeVries CJ, Noordergraaf A. Analogue studies of the human systemic arterial tree. *Biomechan* 1969; 2: 121-43.
15. Croston RC, Fitzjerrell DG. Cardiovascular model for the simulation of exercise, lower body negative pressure, and tilt table experiments. In: Proceedings of the 5th Annual Pittsburgh Conference on Modeling Simulation. Pittsburgh, PA: 1974; 471-6.
16. Heldet T, Shim E. Modeling of cardiovascular response to orthostatic stress. *J Appl Physiol* 2002; 92: 1239-54.
17. Olufsen MS, Nadim A. On deriving lumped models for blood flow and pressure in the systemic arteries. *Math Biosci Eng* 2004; 1: 61-80.
18. Wang JJ, Parker KH, Wave propagation in a model of arterial circulation. *J Biomech* 2004; 37: 457-70.
19. Urquiza S, Blanco P, Lombera M, Marcelo V, Feijoo R. Coupling multidimensional compliant model for carotid artery blood flow. *J Mecanica Computacional* 2003; 22: 232-43.
20. Guyton AC, Hall JE. Textbook of Medical Physiology. 9th ed. Philadelphia: W.B. Saunders; 1996.
21. Abdolrazaghi M, Navid Bakhsh M, Hassani K. Mathematical modeling of Intra-balloon pumping. *Comput Methods Biomech Biomed Engin* 2009 (In press).
22. Levy JH, Tanaka KA. Inflammatory response to cardiopulmonary bypass. *Ann Thorac Surg* 2003; 75: S715-20.
23. Darovic GO, Stratton KL, Hemodynamic monitoring, invasive and noninvasive clinical application. 3rd ed. Philadelphia: Saunders; 2002.
24. Abdolrazaghi M, Navidbakhsh M, Hassani K. Mathematical modeling of cardiovascular system. *Cardiovascular Eng* 2009 (In press).